




Cite this: *Nanoscale*, 2021, 13, 9147

Extending photocatalysis to the visible and NIR: the molecular strategy

Alexandra Mavridi-Printezi,  Arianna Menichetti,  Moreno Guernelli  and Marco Montalti *

Photocatalysis exploits light to perform important processes as solar fuel production by water splitting, and CO₂ reduction or water and air decontamination. Therefore, photocatalysis contributes to the satisfaction of the increasing needs for clean energy, environmental remediation and, most recently, sanitation. Most of the efficient semiconductor nanoparticles (NP), developed as photocatalysts, work in the ultraviolet (UV) spectral region and they are not able to exploit either visible (Vis) or near infrared (NIR) radiation. This limitation makes them unable to fully exploit the broad band solar radiation or to be applied in indoor conditions. Recently, different approaches have been developed to extend the spectral activity of semiconductor NP, like for example band-gap engineering, integration with upconversion NP and plasmonic enhancement involving also hot-electron injection. Nevertheless, the use of organic molecules and metal complexes, for enhancing the photoactivity in the Vis and NIR, was one of the first strategies proposed for sensitization and it is still one of the most efficient. In this minireview we highlight and critically discuss the most recent and relevant achievements in the field of photocatalysis obtained by exploiting dye sensitization either *via* dynamic or static quenching.

Received 3rd March 2021,

Accepted 22nd April 2021

DOI: 10.1039/d1nr01401c

rsc.li/nanoscale

1 Introduction

Photocatalytic processes exploit light, typically sunlight, to achieve chemical reactions of enormous importance for the human community.¹ These processes can be utilized *e.g.* for storing solar energy in the form of clean and abundant fuel, H₂, starting from water^{2–4} or to convert potentially hazardous pollutants such as CO₂ into useful compounds.^{5–7} In organic synthesis light-driven reactions have much weaker impact on the environment than traditional thermal processes and they can allow a better control on the selectivity.^{8–12} Finally, photocatalysis can be exploited for the removal of chemical and biological contaminants from water and air both in outdoor and indoor conditions.^{13–15}

Photocatalysis is a multistep process where a photoactive system, the photocatalyst (PC), completes, in the simplest case, three sequential processes: (i) photon absorption, (ii) charge separation to produce hole and electrons and (iii) redox reaction with reactants. The overall efficiency is hence, the product of the efficiencies of the three processes. To be more precise, a photocatalytic reaction is a thermodynamically downhill process, while the thermodynamically uphill process with $\Delta G > 0$, like solar fuel production, is a photosynthetic reaction.¹⁶ Nevertheless, in most cases this distinction is not

considered in the scientific literature. The most important photocatalytic processes and in particular solar fuel production, are not only strongly energetically demanding ($\Delta G \gg 0$), but also they require additional energy to overcome the high kinetic energy barriers (over-potentials), even in the presence of co-catalysts. Additionally, as shown in Fig. 1, before the actual available reactive electrons and holes species are formed, part of the energy of the initially absorbed photon is dissipated through relaxation processes. As a consequence, when simple schemes as the one in Fig. 1 are considered, high energy UV photons are typically needed. For example, photocatalytic water splitting with a 96% quantum efficiency was recently reported by Domen and co-workers using aluminium-doped strontium titanate PC under UV light irradiation.¹⁷

Indeed, depending on the application, different spectral signatures are required. In particular, broad spectrum activity, ranging from the UV to the NIR^{18,19} is needed in order to achieve highly efficient exploitation of the whole solar energy spectrum for efficient solar fuel production and environmental remediation. Good efficiency upon Vis light absorption is necessary for most indoor applications involving the use of artificial light sources. PC for organic synthesis need to be responsive to powerful, safe and easily available light source typically in Vis-NIR range.²⁰

In general, the strategies to enhance the response of PC in the Vis and NIR regions can be, to some extent, grouped in few general categories.² Among others, band-gap engineering, inte-

Department of Chemistry "Giacomo Ciamician", Via Selmi 2, 40126 Bologna, Italy.
E-mail: marco.montalti2@unibo.it

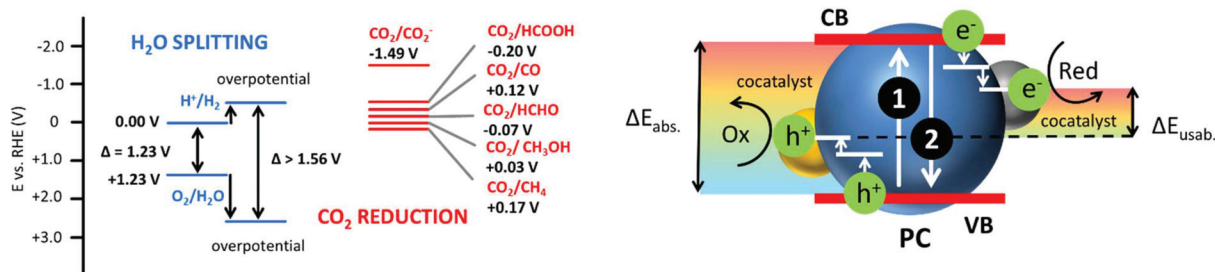


Fig. 1 Left. Simplified energy diagrams for water splitting and CO₂ photoreduction. The actual energy need ΔG for water splitting is only 1.23 V that corresponds to just about 1000 nm and hence to NIR region photons. Nevertheless, the overpotential for this multistep process is considerable and higher energy is needed even in the case of the use of cocatalyst for reduction and oxidation. Additionally, as shown on the right, photon energy is absorbed by the PC (ΔE_{abs}) transferring an electron from the valence band (VB) to the conduction band (CB), therefore producing the electron–hole pair (process 1). Nevertheless, even in the case of poor charge recombination (process 2), several processes occur before the separated and trapped electron are available for the reaction (including charge transfer to the cocatalysts). This reduces the amount of energy actually available for redox (ΔE_{usab}).

gration with up-conversion NP and plasmonic enhancement²¹ involving also hot-electron injection,²² are included. The use of molecular photosensitizers (PS), as those shown in Fig. 2, was proposed for extending the spectral response of photocatalytic systems since four decades, nevertheless this approach is still one of the most efficient.²³ The most recent and promising approaches for molecular based sensitization include the incorporation of the PS in the PC nanostructure, especially in the case of Metal Organic Framework (MOF)²⁴ or Covalent Organic Framework (COF),²⁵ or the exploitation of multiple sequential photon absorption.²⁶ Depending on the strategy, the PS can be either (i) integrated in the PC, (ii)

bound covalently or non-covalently to PC or can be (iii) free in solution. In the first two cases, during the excitation the PS is already “interacting” with the PC and the excited PS is quenched by the PC “statically”, typically *via* electron transfer.²⁷ In the third case, the free PS is excited and then it diffuses toward the PC creating some delay between excitation and sensitization through the “dynamic” process. As a drawback, relatively long excited state lifetimes are requested for the dynamic sensitization. On the other hand, back-diffusion after electron injection can lead to kinetic stabilization of the charge separated pair, while in the case of static processes, fast charge recombination typically occurs, unless charge



Alexandra Mavridi-Printezi (right), Arianna Menichetti (left) and Moreno Guernelli (center)

Alexandra Mavridi-Printezi (right), Arianna Menichetti (left) and Moreno Guernelli (center) are PhD students in the group of Prof. Marco Montalti. Their main research activity is the development of organic and inorganic photoactive supramolecular and/or nanostructured platforms for energy conversion, environmental remediation and ROS photogeneration. The materials on which their research projects are focused include metal–oxide and metal nanoparticles, graphene and related materials, organic chromophores and melanin-like NP.



Marco Montalti

Marco Montalti received his PhD in Chemical Sciences in 2001 and he is presently Professor of Chemistry at the University of Bologna. In 2002 he started his independent research career in the field of luminescent silica and metal nanoparticles for sensing and bioimaging. The main research topics of his group are the design, production, and characterization of Vis-NIR photoactive and/or stimuli responsive supramolecular and nanostructured systems and nanocomposites. Applications of these materials include photocatalysis for energy conversion and environmental remediation, bioimaging and theranostic.



Fig. 2 Examples of PS molecules covering the Vis-NIR absorption window. The optical properties can be finely tuned by changing the substituents or the central metal (in the case of porphyrins, phthalocyanines and naphthalocyanines). The choice of the substituents affects also the solubility, aggregation properties, and the interaction with the different photocatalytic materials.

migration and stabilization takes place (also involving cocatalysts).⁶

In addition, as shown in Fig. 3, sensitization occurs, in the simplest case, *via* electron injection from the excited PS to the PC VB producing the oxidized PS. Often sacrificial agents (*e.g.* triethanol amine, TEOA) are used to restore the PS but this actually alters the energetic balance of the overall photocatalytic process. As a result, for a better exploitation of the energy of Vis-NIR photons, more sophisticated photocatalytic schemes involving multiple photon (sequential) absorption, as the Z-scheme shown in Fig. 3, are necessary.

Another parameter that has to be considered in photocatalysis is oxygen, that is typically present in the reaction environment, and which can quench the PS or be involved in alternative photocatalytic cycles.²⁸

Going back to spectral sensitivity, as shown in Fig. 2, the optical properties of the molecular PS are strongly affected by the presence of substituents. Interestingly the effect of substitution can be, to a large extent predicted, by computational chemistry.^{29,30} Recently it was, for example, demonstrated as a slight difference in the structure, as the one between chlorophyll and bacteriochlorophyll, results in substantial shift of the absorption energy.^{31,32}

Even though one of the main challenges in photocatalysis is the development of materials that exploit light energy more and more efficiently, it is still difficult to univocally quantify this efficiency and its dependency on the irradiation wavelength.³³

Considering for example the definition of quantum efficiency or quantum yield of a photoreaction³⁴ it may appear

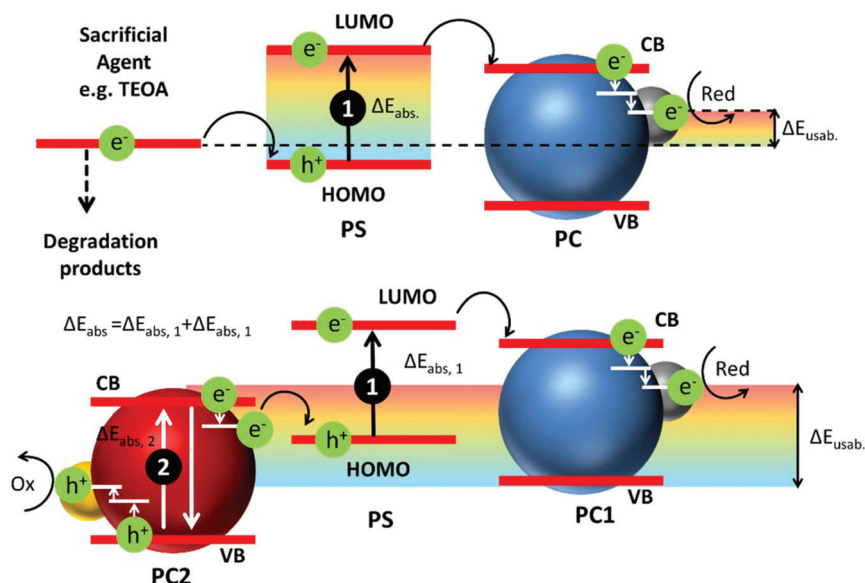


Fig. 3 Top. A molecular PS can absorb photon of lower energy with respect to the PC and then inject an electron into the CB of the PC that then can perform reduction. Differently from the direct excitation of the PC sensitization does not produce h^+ in the PC but in the oxidized PS (PS^+). If a sacrificial agent is used for reducing the PS, its degradation has to be considered in the energetic balance, reducing the actual amount of usable energy. Bottom. An effective way to achieve more energetic processes is the combination of the energy of two photon absorbed by the PS (process 1) and by a second PC (PC2, process 2) in a Z-scheme.

surprising that a PC can, in principle, absorb light poorly at a given wavelength showing a high quantum efficiency anyway. For this reason, new definitions have been introduced to consider the effect of the wavelength as the apparent quantum yield or, specifically for hydrogen production, the solar-to-hydrogen efficiency (STH).² Nevertheless, the actual comparison of results from different research groups is still in many cases very difficult, especially when multiple photon absorption is involved, where the efficiency of the process becomes dependent on the irradiation intensity and the spectral distribution.

In this minireview we will focus on the role of molecular PS in photocatalysis as a strategy able to extend the spectral activity of PC in the Vis and NIR region. We would like to underline that, also considering the vastity of this topic, in this work we do not aim to give a comprehensive overview of the scientific production in the field, but rather to present briefly a selection of the most recent and interesting developments, focussing on different materials used either in heterogeneous or homogeneous photocatalysis.

2 Heterogeneous photocatalysis

Several different semiconductors have been proposed for heterogeneous photocatalysis. A large number of them is very effective upon UV exposure, but they show poor photocatalytic efficiency upon irradiation in the Vis or in the NIR.

2.1 Metal oxide NP

Most metal oxide semiconductor NP, and in particular TiO₂, are efficient photocatalysts under UV irradiation, but because of their broad electronic band gap they do not absorb Vis light.² Structure modification by hydrogenation and reduction treatments, to produce “black” TiO₂, contributed only in part to the increase of the Vis-driven photocatalytic activity.³⁵ In fact, this activity of inorganic semiconductor NP in the Vis-NIR can be enhanced by conjugating them either to up-conversion nanoparticles (UCNP) or to plasmonic metal structures.^{36–38}

Sensitization with inorganic quantum dots and carbon or graphene dots has been also reported.³⁹ Moreover, the successful application of metal oxide as PC for solar light based H₂ photogeneration,^{2,40} CO₂ photoreduction, environmental remediation and organic synthesis have been described bibliographically.^{41,42} It must be noted that the sensitization of TiO₂ by ruthenium(II) trisdiimine complexes (in particular [Ru(bpy)₃]²⁺, bpy = 2,2'-bipyridine) in order to achieve photocatalytic H₂ production under Vis light was already reported in 1981.²³ More recently, various dyes, including diketopyrrolopyrrole,⁴³ phenothiazine derivatives,⁴⁴ phenoxazine and carbazole derivatives,⁴⁵ as well as perylene monoimide,⁴⁶ have been immobilized on semiconductors.

An interesting alternative to conventional photosensitization was recently proposed by Wurthner and Xie (Fig. 4), who developed a TiO₂ modified PC⁴⁷ for hydrogen evolution based on a sequential dual photon absorption according to a scheme previously proposed by König and coworkers.^{48,49} The PC was obtained by grafting to TiO₂ NP a perylene bisimide (PBI) dye able to absorb green light, forming a stable radical anion. The previously formed species could absorb in a second step NIR giving finally, a stable PBI dianion. In a further stage, the dianion absorbed red light photons and, once excited, injected an electron into the TiO₂ NP leading to hydrogen evolution at a rate as high as 1216 μmol h⁻¹ g⁻¹. Being still under discussion,⁵⁰ this mechanism has been recently investigated by ultrafast transient spectroscopy.⁵¹

A different PBI was also proposed by Bonchio and Prato as a PS for achieving the most critical step of water splitting, the water photo-oxidation to produce oxygen.⁵² More in detail, a photo-anode, that was able to mimic the natural photosystem II, was constructed by the functionalization of nano-WO₃ with a hierarchically organized PBI/polyoxometalates (POM)⁵³ system. In this system the formation of large two-dimensional paracrystalline domains was observed and a light-harvesting efficiency higher than 40%, with a peak quantum efficiency under green light irradiation (λ > 500 nm), was demonstrated.

In another interesting example, Huang and Liu adopted also a supramolecular approach in order to expand the photo-

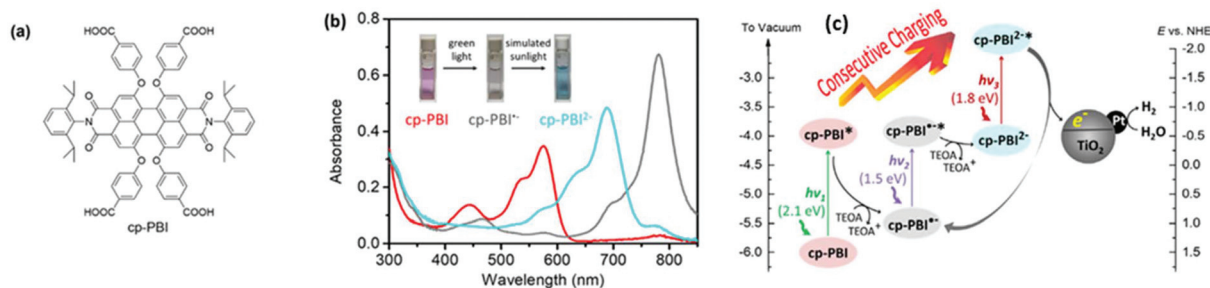


Fig. 4 (a) Illustration of the chemical structure of PBI dye. (b) UV/Vis absorption spectra of PBI in the absence of oxygen and in the presence of sacrificial thioethanolamine in the dark, and of its two anion forms produced by light irradiation in the presence of the same sacrificial agent. Inset in (b) exhibits the images of the solutions in cells. (c) Schematic representation of the hydrogen evolution including the charging processes of PBI through multistep photo-induced electron transfer and the upcoming charge transfer from the PBI dianion to TiO₂ NP. The positions of the energy levels for both radical anion and the dianion are estimated based on the cyclic voltammetry results. Normal hydrogen electrode is symbolized as NHE. This figure has been reproduced from ref. 47 with permission from John Wiley and Sons, copyright 2020.

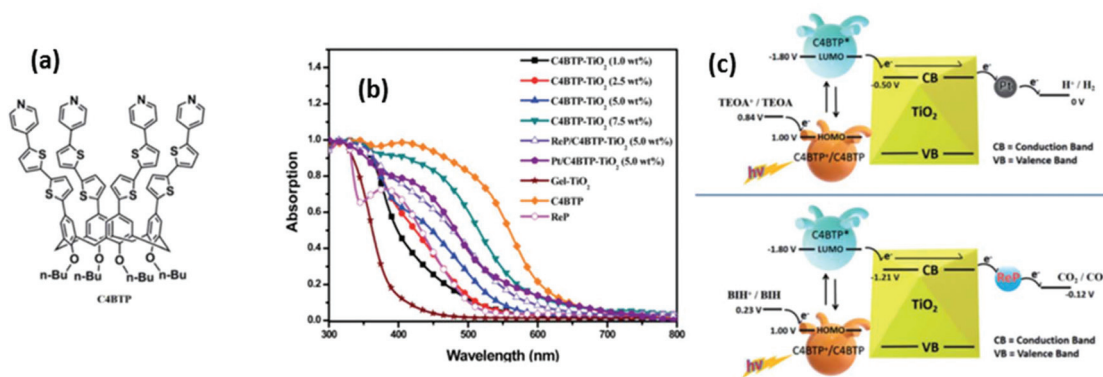


Fig. 5 (a) Chemical structure of calix[4]arene-based dye. (b) UV-Vis absorption spectra of calix[4]arene dye, gel-TiO₂, and dye-TiO₂ with different content of the first (c) Illustration of the band structure and total mechanism of the system for (top) H₂ evolution in water solution and (bottom) CO₂ reduction of calix[4]arene -TiO₂ in DMF solution. All the potential noted are against normal hydrogen electrode (NHE). This figure has been reproduced from ref. 54 with permission from Royal Society of Chemistry, copyright 2020.

catalytic efficiency of TiO₂ in the Vis region. In this case, TiO₂ NP, after being functionalized with a new calix[4]arene dye, were loaded with a rhenium complex Re(bpy)(CO)₃Cl for CO₂ reduction to CO (Fig. 5).⁵⁴

Targeting the same photocatalytic process Meyer and co-workers functionalized NiO NP, using a Zr⁴⁺ based layer-by-layer procedure and a phosphonate derivative of [Ru(bpy)₃]²⁺, in order to produce a donor-chromophore-catalyst assembly for the photoreduction of CO₂ to CO.⁵⁵

Inorganic semiconductor nanomaterials offer as major advantages high chemical and photochemical stability and a relatively high efficiency of the charge separation process with the formation of long-lived reactive species suitable for solar fuel production. Nevertheless, it is worth considering that in the case of photosensitization the stability of the PS itself may become a major concern and the long term efficiency of hybrid organic PS/inorganic semiconductor in the Vis-NIR region has not been clearly explored yet.

2.2 Perovskites

The use of metal halide perovskite (MHP) in photocatalysis is limited⁵⁶ mostly because of their poor stability and of the fast electron-hole recombination.^{57,58} Although several strategies have been proposed to overcome these obstacles^{2,56,59,60} it is worth noticing that even in the case of perovskite-based PC the use of a molecular PS can allow their easy integration in a Z-scheme by coupling two photocatalytic processes, as recently demonstrate for overall water splitting (Fig. 6).⁶¹

2.3 2D Materials

2D materials like graphene,^{62,63} TMDs,^{64,65} MXenes⁶⁶ and black phosphorus absorb efficiently Vis/NIR light and they have been extensively used for Vis-NIR photocatalysis.¹⁵ However, these materials are either conductors or they show fast recombination of the photo-generated electron-hole pair, therefore they found application in photocatalysis mostly as cocatalysts.^{6,41}

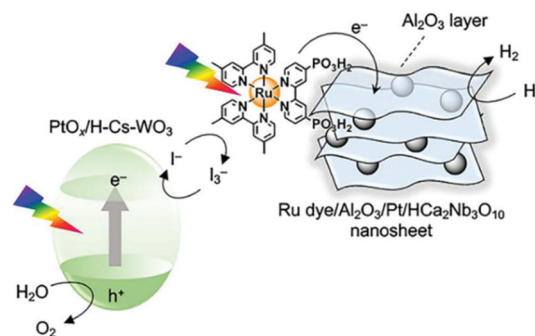


Fig. 6 Schematic illustration of Z-scheme splitting using Ru(II) tris-diimine dye for sensitization of Al₂O₃/Pt/HCa₂Nb₃O₁₀ nanosheets in combination with PtO_x/H-Cs-WO₃. This figure has been reproduced from ref. 61 with permission from American Chemical Society, copyright 2020.

Recently, graphitic carbon nitride (g-CN) on the contrary, has found wide application as PC.⁶⁷

Graphene. Recent attempts to open the band gap of graphene in order to exploit it as PC, include nitrogen doping and production of graphene quantum.⁶⁸ In this last case, sensitization with rhodamine was utilized for H₂ generation.⁶⁹

MXene. Thanks to its 2D structure and electronic conductivity, MXene was recently exploited as an electronic acceptor able to favor the charge separation in semiconductors, recalling the role of graphene.^{70,71} In particular, MXenes were used as co-catalysts for Vis-NIR based H₂ production in combination with COFs,⁷² CdS nanorods⁷³ or Pt NP.⁷⁴ On the other hand, sensitization with molecular PS has been rarely documented. A recently reported exception was the use of Eosin Y for the sensitization of a TiO₂/Ti₃C₂ composite on amorphous carbon.⁷⁵

Black phosphorus. Differently from other phosphorous-based materials,⁷⁶⁻⁷⁸ black phosphorous (BP) is a 2D material with a bandgap (0.3–1.5 eV) dependent on the number of layers.⁷⁹ However, even if BP absorbs Vis/NIR, its photocatalytic efficiency is still low and its quantum efficiency has

not been extensively studied yet.^{80,81} BP is almost always associated with other materials in order to be competitive for photocatalytic applications.^{82,83} For example H₂ production under Vis/NIR irradiation was achieved by 2D/2D heterojunction of BP and carbon nitride (BP/g-CN)⁸⁴ and either by combination with CdS NP⁸⁵ or with MoS₂-BP/GO.⁸⁶

Similarly to MXene, BP was rarely sensitized with molecular PS. A recent example was presented by Xue *et al.*, who suggested an Erythrosin B-sensitized system, using BP/Pt as a co-catalyst for photocatalytic H₂ production under Vis light irradiation.⁸⁷

Graphitic carbon nitride (g-CN). This organic semiconductor exhibits Vis light response, because of its narrow and tunable band gap and an excellent chemical stability.⁶⁷ Among the strategies proposed, in order to increase the small surface, reduce the high electron-hole recombination and tune the optical properties of this material, are included non-metal doping, thermal exfoliation, carbon-dots functionalization^{88,89} and more recently incorporation into heterojunction.⁶⁷ All these strategies aimed to the production of PC suitable for solar water splitting,⁹⁰ CO₂ reduction,^{38,91,92} environmental remediation^{18,93} and organic synthesis.^{94–96}

In the past, several light-harvesting units have been exploited to extend the spectral activity of g-CN, such as Eosin Y,⁹⁷ phthalocyanine,^{98–100} and porphyrin.^{101–104}

Da Silva and co-workers sensitized g-CN by means of free-based porphyrins to promote H₂ production under UV-Vis irradiation.¹⁰⁵ Moreover, several metalloporphyrins can be used as PS in carbon nitride for H₂ production.¹⁰⁶ However, porphyrin often has a double role in the enhancement of g-CN photocatalytic activity, behaving both as PS and co-catalyst by inhibiting charge recombination.^{107–111} Resiner, in particular developed a system where a polymeric cobalt phthalocyanine was used to functionalize g-CN working purely as a co-catalyst for CO₂ reduction.¹¹²

g-CN sensitization by phthalocyanine was applied also for H₂ production. For this purpose, Zeng *et al.* exploited a zinc phthalocyanine¹¹³ and Yi *et al.* a copper phthalocyanine.¹¹⁴

Moving toward different examples, Yuan *et al.* enhanced the photocatalytic water oxidation under Vis light by using 3,4,9,10-perylenetetracarboxylic acid anhydride as a sensitizer.¹¹⁵ In another interesting example, Chlorine e6 was used as a NIR biosafe PS.¹¹⁶ The resulting system had absorbance within 200–1400 nm and could be suitable in energetic, environmental and biological applications.

In a late work, oxidized g-CN rich in hydroxyl and carboxyl functional groups was selected as a support, able to bind with multiporphyrin arrays *via* a layer-by-layer assembling to achieve a nanocomposite, that eventually exhibited dramatic photocatalytic Vis-light degradation of Rhodamine B and phenol.¹⁰⁸ Although g-CN is surely a promising material for Vis-NIR based photocatalysis both for its intrinsic low band gap, chemical composition, simplicity of preparation and low cost, it still has not been demonstrated to be competitive with respect to inorganic semiconductor in term of charge separation efficiency and long term stability.

2.4 Metal organic frameworks (MOF)

Metal-organic frameworks (MOF), also known as porous coordination polymers, have been applied effectively for a variety of Vis light-activated processes like H₂ production,^{117,118} CO₂ photo-reduction,^{119–121} photo-degradation of dyes and pollutants,^{122,123} disinfection of bacteria¹²⁴ and various organic reactions.^{125,126} Advantages of MOF include the presence of pores for selective introduction of substrates,²⁴ easy modification for single atom catalysis¹²⁷ and bandgap tunability with plasmonic NP.¹²⁸ On the other hand, main concerns are the moderate water stability of MOF¹²⁹ and the low mobility of photogenerated electrons and holes.¹³⁰ Unfortunately, numerous MOF exhibit optical absorption only in the UV region.²⁴ A simple and effective molecular strategy in order to overcome the aforementioned obstacles, and therefore tune the optical properties, is based on the choice of the ligands, which can act as an ‘incorporated’ light-absorbing antenna exploiting ligand to metal charge transfer (LMCT) processes.^{124,131,132} Another possibility is the use of an ‘external’ photosensitizers (PS) either *via* dynamic or static quenching.⁴

An interesting example of the first strategy was recently proposed by Cadiou *et al.* who exploited a titanium MOF containing a pyrene derivative as Vis light-responsive photocatalyst for a range of reactions including hydrogen evolution (Fig. 7a).¹³³ Isaka *et al.* developed a set of titanium based MOF with different organic ligands able to absorb light up to 500 nm and they demonstrated their applicability for the photocatalytic synthesis of hydrogen peroxide in a two phase system.¹³⁴

Dynamic sensitization was proposed by Wang *et al.* in the case of three isostructural MOF, namely MOF-Ni, MOF-Co, and MOF-Cu, which were used in combination with the PS [Ru(bpy)₃]²⁺ for enhanced Vis absorption. In particular, due to the matched LUMO positions between the two components, the photogenerated electrons in the LUMO of the PS could migrate to the surface of the MOF-based catalyst, eventually leading to effective CO₂ reduction with selectivity up to 97.7% in the case of MOF-Ni (Fig. 7b).¹³⁵ Similarly Xu *et al.* suggested a NH₂-MIL-101(Fe) MOF-derived hybrid hollow metal phosphide with high photocatalytic activity and with a H₂ evolution rate up to 13.81 mmol g⁻¹ h⁻¹ upon Eosin Y sensitization.¹³⁶ A recent case of static photosensitization was reported for Rhodamine B, which was exploited as a PS, able to improve the photocatalytic capacity of MIL-125(Ti). The dye could be strongly anchored on the surface of the MOF leading to 90% efficient MO degradation under Vis light *via* hole and superoxide free radical generation.¹³⁶ Similarly, Li *et al.* encapsulated different dyes (Basic Yellow 24, Basic Red 14 and Methylene Blue) to Cu-MOF, with significantly lowered energy band gap values and enhanced photodegradation ability up to 97.3%.¹³⁷

Recently porphyrinic Zirconium MOF have also been demonstrated to be efficient visible light activated PC for PET-RAFT polymerization.¹³⁸ MOF are very versatile structures in which molecular PS can be easily integrated to extend the spectral

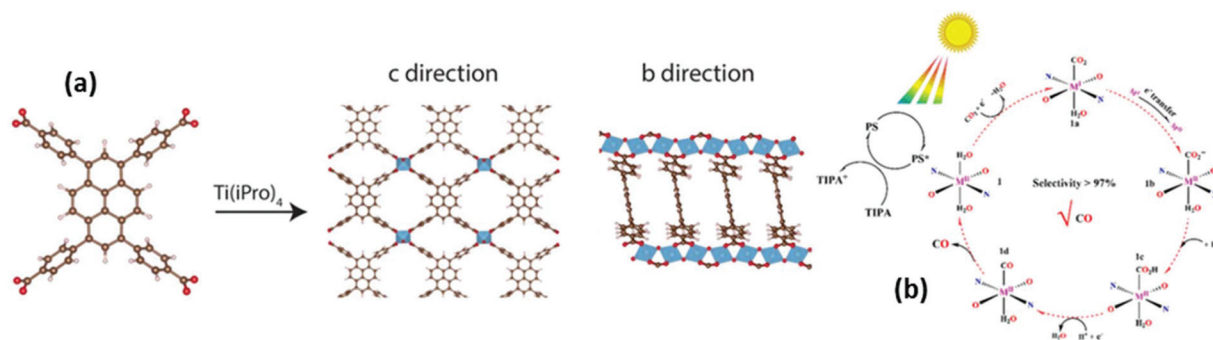


Fig. 7 (a) Schematic illustration of the one-step synthesis of the titanium-based MOF from the 4,4',4''-(pyrene-1,3,6,8-tetrayl)tetrabenzoic acid ligand. In the c direction there are views of the stimulated structure emphasizing on the microporous channels, while in the b direction the views of the Ti–O–Ti chains along the b axis are presented. Ti is illustrated with blue colour, C with dark brown and O with red. H atoms are excluded. (a) This figure has been reproduced from ref. 133 with permission from John Wiley and Sons, copyright 2020. (b) Proposed photocatalytic mechanism of MOFs in the presence of PS for the CO₂ photoreduction to CO. (b) This figure has been reproduced from ref. 135 with permission from American Chemical society, copyright 2019.

responsivity to the Vis-NIR window. Although, the chemical stability of these materials is still a major concern together with the poor charge mobility and electron/hole separation efficiency.

2.5 Covalent organic framework (COF) and conjugated organic polymers (COP)

Covalent organic frameworks (COF) are polymers with tunable porosity, π -conjugated structure, and good chemical stability used for Vis light-based water splitting, CO₂ photo-reduction, dye degradation, and organic synthesis.^{16,25,139–143}

Even though COF are semiconductor materials, their design is based on a molecular approach, and the photophysical and photochemical properties strongly depend on the choice of the incorporated molecular building blocks: triazine, pyrene, porphyrin, thiophene, or sulfone, *etc.*¹⁴⁴ An interesting strategy, able to promote efficiency of photo-generated electron-hole pairs, avoid recombination of charge, and improve light harvesting ability, was achieved by Li *et al.* by the introduction of electron D–A (donor–acceptor) molecular moieties in COF for sunlight-driven H₂ evolution (Fig. 8).¹⁴⁵

In a different approach a molecular PS, [Ru(bpy)₃]²⁺, was incorporated in the pores of a new water-soluble 3D COF together with POM to achieve H₂ photoproduction.¹⁴⁶

Integration of a Re(bpy)(CO)₃Cl homologous in the structure of a crystalline COF was exploited by Fu *et al.* for highly specific Vis photo-conversion of CO₂ into fuels.¹⁴⁷ In another case, in order to extend the spectral activity of terpyridyl-based, 2D lamellar COF-909 nanorods coordination to copper was applied by Dong *et al.*¹⁴⁸ The added metal centers enhanced also the electrons-holes separation providing specific binding sites, able to improve the recognition of target organic toxicants.

An interesting synthetic approach of COF was achieved by Yu *et al.* by polymerizing an Eosin Y precursor (Fig. 9) in a conjugated structure that exhibited high activity for the photocatalytic reduction of CO₂ to CO in the presence of gaseous H₂O.¹⁴⁹ Importantly, the production rate was up to 33 μmol

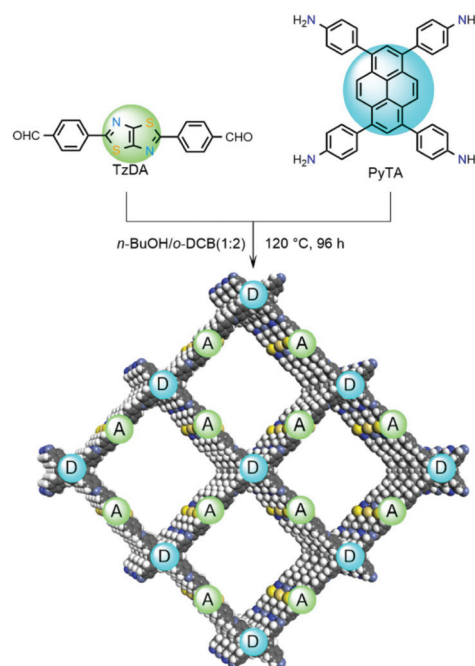


Fig. 8 Donor–Acceptor (D–A) MOF system synthesized under solvothermal condition. This figure has been reproduced from ref. 145 with permission from John Wiley and Sons, copyright 2021.

$\text{g}^{-1} \text{h}^{-1}$ and the selectivity as high as 92%. A rational design of COF, reported by Kang *et al.*, allowed to combine programmed spectral sensitivity to photocatalytic selectivity in organic synthesis. These authors were the first who showed an example of Vis light-driven asymmetric photocatalysis.¹⁵⁰ As for other polymeric materials, because of the lack of a crystalline structure, photo-induced charge separation and migration is poorly efficient in COF and COP. Nevertheless, this drawback is partially compensated by the high versatility of design that allows the simple tuning of the optical properties by incorporating specific molecular absorbers.

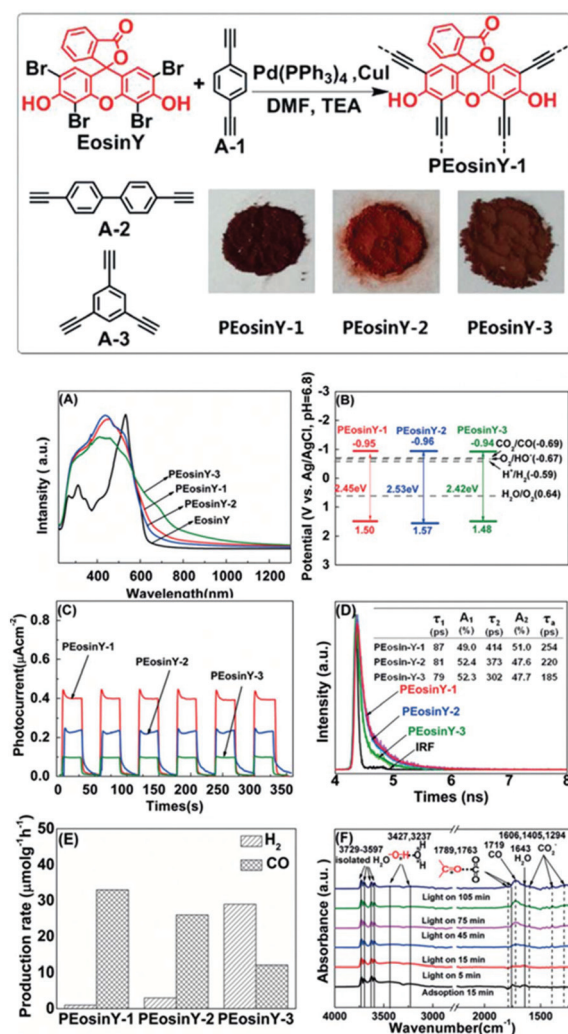


Fig. 9 (Top) Synthetic pathway for the production of the conjugated Eosin Y-functionalized COFs. (A) UV-Vis absorption spectra of Eosin Y and of the Eosin Y functionalized polymers, PEosin Y-N, where $N = 1-3$ (B) Schematic illustration of CB and VB of PEosin Y-N (C) Transient photocurrent responses of PEosin Y-N at $\lambda > 420$ nm (D) time-resolved fluorescent decay spectra (TRFDS) of PEosin Y-N at 640 nm upon irradiation at 405 nm (E) average production rates of CO from CO₂ photoreduction in the presence of PEosin Y-N for 50 h at $\lambda > 420$ nm (F) reflectance infrared Fourier transform spectra (DRIFT) of PEosin Y-N for CO₂ and H₂O absorption and their photoreactions under Vis light irradiation. The bands with significant changes are represented with full lines referring to the decreasing or gradually disappearing bands, and with dashed lines referring to the newly appearing or increasing bands. This figure has been reproduced from ref. 149 with permission from John Wiley and Sons, copyright 2019.

3 Homogeneous photocatalysis

In homogeneous photocatalysis photochemical reactions are typically initiated by the absorption of light by a molecular PS in the reaction solvent.⁹

The excited PS is hence involved either in single electron transfer (SET), in the case of photoredox catalysis, or triplet energy transfer (EnT) *via* Dexter mechanism schematized in



Fig. 10 Simplified schematic illustration of the concept of photocatalysis. This figure has been reproduced from ref. 10 with permission from Royal Society of Chemistry, copyright 2018.

Fig. 10.^{8,10,151} Recently, special attention have been devoted to a more general understanding of the role of singlet and triplet excited states in photoredox catalysis.¹⁵² Advantages of using Vis-NIR light for photoexcitation include: (i) use of light sources safer than UV, (ii) reduced photodamage of the PS, (iii) increased selectivity and (iv) for NIR, the possibility of using non-transparent reaction vessels. The main strategies to exploit the Vis-NIR region in homogenous photocatalysis are two and namely: (i) development of new PS and (ii) multiphoton (sequential) absorption.²⁶ Regarding the former strategy, the efficiency in specific spectral regions depends on the optical properties of the PS itself. Typically used PS, like [Ru(bpy)₃]²⁺ and [Ir(ppy)₃]⁺, absorb only partially in the Vis region ($\lambda < 500$ nm) possessing a moderate molar absorption coefficient ($\epsilon \sim 10^3-10^4$ M⁻¹ cm⁻¹). The search for new PS with enhanced absorption in the Vis-NIR is hence very active. Castellano for example recently proposed a new cyclometalated Ir(III) diimine PS for homogeneous photocatalytic hydrogen production under Vis light.¹⁵³

At the same time the number and variety of chemical processes that can be achieved with Vis-NIR active PS is impressively increasing. Recent examples of visible light driven photocatalysis include, for example, direct isotopic carboxylate exchange of C(sp³) acids with labeled CO₂.¹⁵⁴ Strong bis-cyclometalated iridium PS with electron-rich b-diketiminato ancillary ligands were demonstrated to yield efficient photoredox transformations of unactivated substrates using blue or green visible-light.¹⁵⁵

Synthesis of unnatural α -amino acids *via* stereoselective C-radical addition to a chiral glyoxylate-derived *N*-sulfinyl imine was achieved by visible light-promoted photoredox catalysis using either metal-bases and metal-free PS.¹⁵⁶

A novel strategy was also proposed where CO₂ released by decarboxylation of amino acids (a typical waste byproduct) was used for photoredox-neutral carbocarboxylation of alkenes.¹⁵⁷

In general, large scale application of photocatalysis needs largely available, inexpensive PS that do not contain precious metal.

For this reason Chen *et al.* developed a new strong Vis-light-absorbing copper-based PS with an ϵ as high as 160 000 M⁻¹ cm⁻¹ at 518 nm.¹⁵⁸ By adopting a through-bond energy transfer from boron dipyrromethene (Bodipy) the excitation efficiency of Cu(I) complex was 62 times enhanced. In another important development, Zhang *et al.* proposed a zirconium(IV) PS with ligand-to-metal charge-transfer excited states and

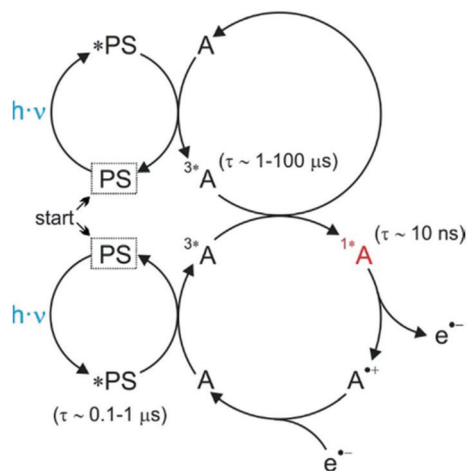


Fig. 11 Schematic illustration of photoredox catalysis via sensitized triplet-triplet annihilation upconversion. The photosensitizer is symbolized as PS, while the annihilator as A. This figure has been reproduced from ref. 26 with permission from John Wiley and Sons, copyright 2020.

demonstrated its applicability for photoredox catalysis. This Zr complex showed a broad absorption band, centered at 525 nm, and an exceptionally long-lived triplet LMCT excited state ($\tau = 350 \mu\text{s}$), featuring highly efficient photoluminescence emission ($\Phi = 0.45$) and a peculiar delayed fluorescence.¹⁵⁹

Regarding the development of new PS, it is worth underlining that absorption of low energy photons produces excited state with poor energy content, hardly exploitable for most valuable chemical reactions. Consequently, the combination of photons of low energy to produce high energy species, in new photocatalytic scheme is surely a promising strategy.²⁶ In this context, some years ago the reduction of aryl halides by consecutive Vis light-induced electron transfer processes was reported.⁴⁸ The photocatalytic mechanism was investigated more in detail by the group of Schanze.⁵¹

In alternative, the sequential absorption of two low energy photons has been recently proposed for example by Ravetz *et al.* who demonstrated that molecules absorbing infrared light can be used for photoredox catalysis exploiting triplet fusion upconversion (Fig. 11); a process that transforms two low energy poorly reactive triplet excited states into a high energy reactive one. The resulting system containing a PS and an annihilator is able to accomplish a wide range of photoredox reactions under NIR light illumination.¹⁶⁰ Similarly, Mahammed *et al.* reported triplet-triplet annihilation upconversion for phosphorus corrole complexes.¹⁶¹ Recently, Nicewicz's group demonstrated the formation, upon sequential multiple photon absorption, of a neutral acridine radical with a maximum excited-state oxidation potential similar to elemental lithium.¹⁶²

4 Conclusions and perspective

In this minireview, Vis-NIR activation of PC by using molecular absorbers has been demonstrated to be still a valid approach

almost even after 40 years from its introduction. Indeed, the most recent sensitization strategies exploit both new PC and new PS, but also new synthetic approaches as the incorporation of molecular absorber in the PC structure. Eventually, the development of new PS and new scheme of photoreaction involving multiple photon absorption has been achieved in many cases. In general, the molecular strategy is very direct and can be easily adapted by most PC. On the contrary, a main concern is still the use of PS based on rare transition metal complexes like Ru and Ir. In principle, the materials discussed in this minireview have been demonstrated to be suitable for multiple Vis-NIR based photocatalytic applications, ranging from solar fuel production to environmental remediation. Nevertheless inorganic semiconductor nanostructures demonstrated to be still superior in term of stability and charge separation efficiency and they are still a primary choice for long term use as in the case of platforms for solar energy conversion. On the other hand, materials like MOF and COF can be easily designed to exploit Vis-NIR light and thanks to their porosity and ability of binding target molecules like CO_2 are promising alternative to inorganic semiconductor, although further efforts are required in order to improve their efficiency and stability.

In general, it must be noted that the global scale application, as solar fuel production (from water or CO_2 abatement) or environmental remediation, require a photocatalytic scheme based on low cost, non-toxic materials easily producible on the large scale.⁴⁰ For this materials like g-CN are attracting increasing attention although their photocatalytic properties still need improvement.

Even if less strictly, the above mentioned features are also important in the case of homogenous photocatalysis applied to organic synthesis.

In this context, the use of organic PS and multiphotonic scheme is surely promising. Nevertheless, the long-term stability of organic PS in view of their real application needs still to be demonstrated and reassured. Up to now, the comparison of the actual photocatalytic efficiency of the different systems is complicated by the variety of experimental conditions and in particular, by the use of sacrificial agents, the decomposition of which needs indeed to be considered in the overall energetic storage balance. In general, the efficiencies that have been reported for photocatalytic solar fuel production do not seem to meet the huge energy demands of the modern society, demonstrating how challenging photocatalysis is and the need for even more dedication and effort, also in terms of investment.

Author contributions

A. M.-P., A. M., M. G. and M. M. contributed to the bibliographic search and to the writing of this minireview.

Conflicts of interest

There are no conflicts to declare.

Acknowledgements

This research was funded by the Italian Ministry of Education, University and Research (MIUR), (PRIN project: PRIN 2017) 2017E44A9P (BacHound).

Notes and references

- N. Armaroli and V. Balzani, *Angew. Chem., Int. Ed.*, 2007, **46**, 52–66.
- Q. Wang and K. Domen, *Chem. Rev.*, 2020, **120**, 919–985.
- Z. Wang, C. Li and K. Domen, *Chem. Soc. Rev.*, 2019, **48**, 2109–2125.
- X. Zhang, T. Peng and S. Song, *J. Mater. Chem. A*, 2016, **4**, 2365–2402.
- W. H. Zhang, A. R. Mohamed and W. J. Ong, *Angew. Chem., Int. Ed.*, 2020, **59**, 22894–22915.
- X. Li, J. G. Yu, M. Jaroniec and X. B. Chen, *Chem. Rev.*, 2019, **119**, 3962–4179.
- S. C. Shit, I. Shown, R. Paul, K. H. Chen, J. Mondal and L. C. Chen, *Nanoscale*, 2020, **12**, 33.
- Q. Q. Zhou, Y. Q. Zou, L. Q. Lu and W. J. Xiao, *Angew. Chem., Int. Ed.*, 2019, **58**, 1586–1604.
- L. Buzzetti, G. E. M. Crisenza and P. Melchiorre, *Angew. Chem., Int. Ed.*, 2019, **58**, 3730–3747.
- F. Strieth-Kalthoff, M. J. James, M. Teders, L. Pitzer and F. Glorius, *Chem. Soc. Rev.*, 2018, **47**, 7190–7202.
- S. Crespi and M. Fagnoni, *Chem. Rev.*, 2020, **120**, 9790–9833.
- Y. S. Jiang and E. A. Weiss, *J. Am. Chem. Soc.*, 2020, **142**, 15219–15229.
- X. Pang, N. Skillen, N. Gunaratne, D. W. Rooney and P. K. J. Robertson, *J. Hazard. Mater.*, 2021, **402**, 123461.
- A. H. Mamaghani, F. Haghghat and C. S. Lee, *Build. Environ.*, 2021, **189**, 11.
- G. Guidetti, E. A. A. Pogna, L. Lombardi, F. Tomarchio, I. Polishchuk, R. R. M. Joosten, A. Ianiro, G. Soavi, N. A. J. M. Sommerdijk, H. Friedrich, B. Pokroy, A. K. Ott, M. Goisis, F. Zerbetto, G. Falini, M. Calvaresi, A. C. Ferrari, G. Cerullo and M. Montalti, *Nanoscale*, 2019, **11**, 19301–19314.
- T. Banerjee, F. Podjaski, J. Kroger, B. P. Biswal and B. V. Lotsch, *Nat. Rev. Mater.*, 2021, **6**, 168–190.
- T. Takata, J. Jiang, Y. Sakata, M. Nakabayashi, N. Shibata, V. Nandal, K. Seki, T. Hisatomi and K. Domen, *Nature*, 2020, **581**, 411–414.
- S. Zhang, P. C. Gu, R. Ma, C. T. Luo, T. Wen, G. X. Zhao, W. C. Cheng and X. K. Wang, *Catal. Today*, 2019, **335**, 65–77.
- Q. Tian, W. Yao, W. Wu and C. Jiang, *Nanoscale Horiz.*, 2019, **4**, 10–25.
- N. Corrigan, J. Yeow, P. Judzewitsch, J. Xu and C. Boyer, *Angew. Chem., Int. Ed.*, 2019, **58**, 5170–5189.
- X.-C. Dai, M.-H. Huang, Y.-B. Li, T. Li, S. Hou, Z.-Q. Wei and F.-X. Xiao, *J. Phys. Chem. C*, 2020, **124**, 4989–4998.
- N. N. Vu, S. Kaliaguine and T. O. Do, *ChemSusChem*, 2020, **13**, 3967–3991.
- E. Borgarello, J. Kiwi, E. Pelizzetti, M. Visca and M. Grätzel, *Nature*, 1981, **289**, 158–160.
- Q. Wang and D. Astruc, *Chem. Rev.*, 2020, **120**, 1438–1511.
- Q. Yang, M. L. Luo, K. W. Liu, H. M. Cao and H. J. Yan, *Appl. Catal., B*, 2020, **276**, 18.
- F. Glaser, C. Kerzig and O. S. Wenger, *Angew. Chem., Int. Ed.*, 2020, **59**, 10266–10284.
- M. Montalti, A. Credi, L. Prodi and M. T. Gandolfi, *Handbook of Photochemistry*, 3rd edn, Taylor & Francis, 2006.
- C. Wu, K. Jung, Y. Ma, W. Liu and C. Boyer, *Nat. Commun.*, 2021, **12**, 478.
- C. Wu, H. Chen, N. Corrigan, K. Jung, X. Kan, Z. Li, W. Liu, J. Xu and C. Boyer, *J. Am. Chem. Soc.*, 2019, **141**, 8207–8220.
- C. Wu, N. Corrigan, C.-H. Lim, K. Jung, J. Zhu, G. Miyake, J. Xu and C. Boyer, *Macromolecules*, 2019, **52**, 236–248.
- S. Shanmugam, J. Xu and C. Boyer, *Angew. Chem., Int. Ed.*, 2016, **55**, 1036–1040.
- S. Shanmugam, J. Xu and C. Boyer, *Chem. Sci.*, 2015, **6**, 1341–1349.
- M. J. Buriak, P. V. Kamat and K. S. Schanze, *ACS Appl. Mater. Interfaces*, 2014, **6**, 11815–11816.
- M. Qureshi and K. Takanabe, *Chem. Mater.*, 2017, **29**, 158–167.
- A. Naldoni, M. Altomare, G. Zoppellaro, N. Liu, S. Kment, R. Zboril and P. Schmuki, *ACS Catal.*, 2019, **9**, 345–364.
- E. Peiris, S. Sarina, E. R. Waclawik, G. A. Ayoko, P. F. Han, J. F. Jia and H. Y. Zhu, *Angew. Chem., Int. Ed.*, 2019, **58**, 12032–12036.
- Z. Hu, Y. Mi, Y. Ji, R. Wang, W. Zhou, X. Qiu, X. Liu, Z. Fang and X. Wu, *Nanoscale*, 2019, **11**, 16445–16454.
- Y. Wang, X. H. Liu, Q. K. Wang, M. Quick, S. A. Kovalenko, Q. Y. Chen, N. Koch and N. Pinna, *Angew. Chem., Int. Ed.*, 2020, **59**, 7748–7754.
- Z. Y. Zhang, C. R. Rogers and E. A. Weiss, *J. Am. Chem. Soc.*, 2020, **142**, 495–501.
- T. Hisatomi and K. Domen, *Nat. Catal.*, 2019, **2**, 387–399.
- A. Y. Meng, L. Y. Zhang, B. Cheng and J. G. Yu, *Adv. Mater.*, 2019, **31**, 1807660.
- W. Zhang, H. He, H. Li, L. Duan, L. Zu, Y. Zhai, W. Li, L. Wang, H. Fu and D. Y. Zhao, *Adv. Energy Mater.*, 2021, **11**, 2003303.
- J. Warnan, J. Willkomm, J. N. Ng, R. Godin, S. Prantl, J. R. Durrant and E. Reisner, *Chem. Sci.*, 2017, **8**, 3070–3079.
- N. Manfredi, B. Cecconi, V. Calabrese, A. Minotti, F. Peri, R. Ruffo, M. Monai, I. Romero-Ocaña, T. Montini, P. Fornasiero and A. Abbotto, *Chem. Commun.*, 2016, **52**, 6977–6980.
- N. Manfredi, M. Monai, T. Montini, M. Salamone, R. Ruffo, P. Fornasiero and A. Abbotto, *Sustainable Energy Fuels*, 2017, **1**, 694–698.
- J. Warnan, J. Willkomm, Y. Farré, Y. Pellegrin, M. Boujtita, F. Odobel and E. Reisner, *Chem. Sci.*, 2019, **10**, 2758–2766.

- 47 Y. C. Xu, J. X. Zheng, J. O. Lindner, X. B. Wen, N. Q. Jiang, Z. C. Hu, L. L. Liu, F. Huang, F. Wurthner and Z. Q. Xie, *Angew. Chem., Int. Ed.*, 2020, **59**, 10363–10367.
- 48 I. Ghosh, T. Ghosh, J. I. Bardagi and B. König, *Science*, 2014, **346**, 725–728.
- 49 L. Zeng, T. Liu, C. He, D. Shi, F. Zhang and C. Duan, *J. Am. Chem. Soc.*, 2016, **138**, 3958–3961.
- 50 M. Marchini, A. Gualandi, L. Mengozzi, P. Franchi, M. Lucarini, P. G. Cozzi, V. Balzani and P. Ceroni, *Phys. Chem. Chem. Phys.*, 2018, **20**, 8071–8076.
- 51 C. J. Zeman, S. Kim, F. Zhang and K. S. Schanze, *J. Am. Chem. Soc.*, 2020, **142**, 2204–2207.
- 52 M. Bonchio, Z. Syrgiannis, M. Burian, N. Marino, E. Pizzolato, K. Dirian, F. Rigodanza, G. A. Volpato, G. La Ganga, N. Demitri, S. Berardi, H. Amenitsch, D. M. Guldi, S. Caramori, C. A. Bignozzi, A. Sartorel and M. Prato, *Nat. Chem.*, 2019, **11**, 146–153.
- 53 S.-L. Xie, J. Liu, L.-Z. Dong, S.-L. Li, Y.-Q. Lan and Z.-M. Su, *Chem. Sci.*, 2019, **10**, 185–190.
- 54 Y. H. Zhong, Y. Lei, J. F. Huang, L. M. Xiao, X. L. Chen, T. Luo, S. Qin, J. Guo and J. M. Liu, *J. Mater. Chem. A*, 2020, **8**, 8883–8891.
- 55 D. Wang, Y. Wang, M. D. Brady, M. V. Sheridan, B. D. Sherman, B. H. Farnum, Y. Liu, S. L. Marquard, G. J. Meyer, C. J. Dares and T. J. Meyer, *Chem. Sci.*, 2019, **10**, 4436–4444.
- 56 H. Huang, B. Pradhan, J. Hofkens, M. B. J. Roeffaers and J. A. Steele, *ACS Energy Lett.*, 2020, **5**, 1107–1123.
- 57 Z. J. Chen, Y. G. Hu, J. Wang, Q. Shen, Y. H. Zhang, C. Ding, Y. Bai, G. C. Jiang, Z. Q. Li and N. Gaponik, *Chem. Mater.*, 2020, **32**, 1517–1525.
- 58 W. J. Yin, B. C. Weng, J. Ge, Q. D. Sun, Z. Z. Li and Y. F. Yan, *Energy Environ. Sci.*, 2019, **12**, 442–462.
- 59 H. Wang, X. Wang, H. Zhang, W. Ma, L. Wang and X. Zong, *Nano Energy*, 2020, **71**, 104647.
- 60 R. Li, X. Li, J. Wu, X. Lv, Y.-Z. Zheng, Z. Zhao, X. Ding, X. Tao and J.-F. Chen, *Appl. Catal., B*, 2019, **259**, 118075.
- 61 T. Oshima, S. Nishioka, Y. Kikuchi, S. Hirai, K. I. Yanagisawa, M. Eguchi, Y. Miseki, T. Yokoi, T. Yui, K. Kimoto, K. Sayama, O. Ishitani, T. E. Mallouk and K. Maeda, *J. Am. Chem. Soc.*, 2020, **142**, 8412–8420.
- 62 K.-Q. Lu, Y.-H. Li, F. Zhang, M.-Y. Qi, X. Chen, Z.-R. Tang, Y. M. A. Yamada, M. Anpo, M. Conte and Y.-J. Xu, *Nat. Commun.*, 2020, **11**, 5181.
- 63 A. H. Cheshme Khavar, G. Moussavi, K. Yaghmaeian, A. R. Mahjoub, N. Khedri, M. Dusek, T. Vaclavu and M. Hosseini, *RSC Adv.*, 2020, **10**, 22500–22514.
- 64 H. Li, X. Jia, Q. Zhang and X. Wang, *Chem*, 2018, **4**, 1510–1537.
- 65 C. K. Sumesh and S. C. Peter, *Dalton Trans.*, 2019, **48**, 12772–12802.
- 66 J. Peng, X. Chen, W.-J. Ong, X. Zhao and N. Li, *Chem*, 2019, **5**, 18–50.
- 67 M. Jourshabani, B. K. Lee and Z. Shariatnia, *Appl. Catal., B*, 2020, **276**, 28.
- 68 C. Bie, H. Yu, B. Cheng, W. Ho, J. Fan and J. Yu, *Adv. Mater.*, 2021, **33**, 2003521.
- 69 D. Dinda, H. Park, H.-J. Lee, S. Oh and S. Y. Park, *Carbon*, 2020, **167**, 760–769.
- 70 J. Pang, R. G. Mendes, A. Bachmatiuk, L. Zhao, H. Q. Ta, T. Gemming, H. Liu, Z. Liu and M. H. Rummeli, *Chem. Soc. Rev.*, 2019, **48**, 72–133.
- 71 X. Xie and N. Zhang, *Adv. Funct. Mater.*, 2020, **30**, 2002528.
- 72 H. Wang, C. Qian, J. Liu, Y. Zeng, D. Wang, W. Zhou, L. Gu, H. Wu, G. Liu and Y. Zhao, *J. Am. Chem. Soc.*, 2020, **142**, 4862–4871.
- 73 R. Xiao, C. Zhao, Z. Zou, Z. Chen, L. Tian, H. Xu, H. Tang, Q. Liu, Z. Lin and X. Yang, *Appl. Catal., B*, 2020, **268**, 118382.
- 74 S. Min, Y. Xue, F. Wang, Z. Zhang and H. Zhu, *Chem. Commun.*, 2019, **55**, 10631–10634.
- 75 Y. Sun, Y. Sun, X. Meng, Y. Gao, Y. Dall'Agnese, G. Chen, C. Dall'Agnese and X.-F. Wang, *Catal. Sci. Technol.*, 2019, **9**, 310–315.
- 76 X. H. Ren, D. Philo, Y. X. Li, L. Shi, K. Chang and J. H. Ye, *Coord. Chem. Rev.*, 2020, **424**, 213516.
- 77 D. Xia, Z. Shen, G. Huang, W. Wang, J. C. Yu and P. K. Wong, *Environ. Sci. Technol.*, 2015, **49**, 6264–6273.
- 78 L. F. Hong, R. T. Guo, Y. Yuan, X. Y. Ji, Z. D. Lin, Z. S. Li and W. G. Pan, *ChemSusChem*, 2021, **14**, 539–557.
- 79 H. Liu, K. Hu, D. Yan, R. Chen, Y. Zou, H. Liu and S. Wang, *Adv. Mater.*, 2018, **30**, 1800295.
- 80 T. Sakthivel, X. Huang, Y. Wu and S. Rtimi, *Chem. Eng. J.*, 2020, **379**, 122297.
- 81 Y. Abate, D. Akinwande, S. Gamage, H. Wang, M. Snure, N. Poudel and S. B. Cronin, *Adv. Mater.*, 2018, **30**, 1704749.
- 82 B. Li, C. Lai, G. Zeng, D. Huang, L. Qin, M. Zhang, M. Cheng, X. Liu, H. Yi, C. Zhou, F. Huang, S. Liu and Y. Fu, *Small*, 2019, **15**, 1804565.
- 83 T. Sakthivel, X. Huang, Y. Wu and S. Rtimi, *Chem. Eng. J.*, 2020, **379**, 122297.
- 84 Q. Zhang, S. Huang, J. Deng, D. T. Gangadharan, F. Yang, Z. Xu, G. Giorgi, M. Palummo, M. Chaker and D. Ma, *Adv. Funct. Mater.*, 2019, **29**, 1902486.
- 85 L. Mao, X. Cai, S. Yang, K. Han and J. Zhang, *Appl. Catal., B*, 2019, **242**, 441–448.
- 86 M. Zhu, M. Fujitsuka, L. Zeng, M. Liu and T. Majima, *Appl. Catal., B*, 2019, **256**, 117864.
- 87 Y. Xue, S. Min and F. Wang, *Int. J. Hydrogen Energy*, 2019, **44**, 21873–21881.
- 88 A. Cadranel, J. T. Margraf, V. Strauss, T. Clark and D. M. Guldi, *Acc. Chem. Res.*, 2019, **52**, 955–963.
- 89 Y. Wang, X. Liu, X. Y. Han, R. Godin, J. L. Chen, W. Z. Zhou, C. R. Jiang, J. F. Thompson, K. B. Mustafa, S. A. Shevlin, J. R. Durrant, Z. X. Guo and J. W. Tang, *Nat. Commun.*, 2020, **11**, 9.
- 90 R. Malik and V. K. Tomer, *Renewable Sustainable Energy Rev.*, 2021, **135**, 110235.
- 91 A. Kumar, P. Raizada, V. Kumar Thakur, V. Saini, A. Aslam Parwaz Khan, N. Singh and P. Singh, *Chem. Eng. Sci.*, 2021, **230**, 116219.

- 92 Y. Zhou, Z. Wang, L. Huang, S. Zaman, K. Lei, T. Yue, Z. a. Li, B. You and B. Y. Xia, *Adv. Energy Mater.*, 2021, 2003159.
- 93 C. Zhang, Y. Li, D. M. Shuai, Y. Shen, W. Xiong and L. Q. Wang, *Chemosphere*, 2019, **214**, 462–479.
- 94 K. R. Reddy, C. V. Reddy, M. N. Nadagouda, N. P. Shetti, S. Jaesool and T. M. Aminabhavi, *J. Environ. Manage.*, 2019, **238**, 25–40.
- 95 C. C. Wang, X. H. Yi and P. Wang, *Appl. Catal., B*, 2019, **247**, 24–48.
- 96 M. Jourshabani, B.-K. Lee and Z. Shariatinia, *Appl. Catal., B*, 2020, **276**, 119157.
- 97 S. Min and G. Lu, *J. Phys. Chem. C*, 2012, **116**, 19644–19652.
- 98 X. Zhang, L. Yu, C. Zhuang, T. Peng, R. Li and X. Li, *ACS Catal.*, 2014, **4**, 162–170.
- 99 X. Zhang, T. Peng, L. Yu, R. Li, Q. Li and Z. Li, *ACS Catal.*, 2015, **5**, 504–510.
- 100 W. Lu, T. Xu, Y. Wang, H. Hu, N. Li, X. Jiang and W. Chen, *Appl. Catal., B*, 2016, **180**, 20–28.
- 101 J. Liu, H. Shi, Q. Shen, C. Guo and G. Zhao, *Green Chem.*, 2017, **19**, 5900–5910.
- 102 S. Mei, J. Gao, Y. Zhang, J. Yang, Y. Wu, X. Wang, R. Zhao, X. Zhai, C. Hao, R. Li and J. Yan, *J. Colloid Interface Sci.*, 2017, **506**, 58–65.
- 103 D. H. Wang, J. N. Pan, H. H. Li, J. J. Liu, Y. B. Wang, L. T. Kang and J. N. Yao, *J. Mater. Chem. A*, 2016, **4**, 290–296.
- 104 D. Yang, M. H. Cao, Q. X. Zhong, P. L. Li, X. H. Zhang and Q. Zhang, *J. Mater. Chem. C*, 2019, **7**, 757–789.
- 105 E. S. Da Silva, N. M. M. Moura, M. Neves, A. Coutinho, M. Prieto, C. G. Silva and J. L. Faria, *Appl. Catal., B*, 2018, **221**, 56–69.
- 106 J. Wang, D. Liu, Q. Liu, T. Peng, R. Li and S. Zhou, *Appl. Surf. Sci.*, 2019, **464**, 255–261.
- 107 S. Tian, S. Chen, X. Ren, R. Cao, H. Hu and F. Bai, *Nano Res.*, 2019, **12**, 3109–3115.
- 108 Y.-j. Yang, B.-w. Sun, D.-j. Qian and M. Chen, *Appl. Surf. Sci.*, 2019, **478**, 1027–1036.
- 109 X. Zhang, L. Lin, D. Qu, J. Yang, Y. Weng, Z. Wang, Z. Sun, Y. Chen and T. He, *Appl. Catal., B*, 2020, **265**, 118595.
- 110 L. Li, G. B. Bodedla, Z. Liu and X. Zhu, *Appl. Surf. Sci.*, 2020, **499**, 143755.
- 111 L. Lin, C. C. Hou, X. H. Zhang, Y. J. Wang, Y. Chen and T. He, *Appl. Catal., B*, 2018, **221**, 312–319.
- 112 S. Roy and E. Reisner, *Angew. Chem., Int. Ed.*, 2019, **58**, 12180–12184.
- 113 P. Zeng, J. Wang, Y. Guo, R. Li, G. Mei and T. Peng, *Chem. Eng. J.*, 2019, **373**, 651–659.
- 114 Y. Yi, S. Wang, H. Zhang, J. Liu, X. Lu, L. Jiang, C. Sui, H. Fan, S. Ai and J. Sun, *J. Mater. Chem. C*, 2020, **8**, 17157–17161.
- 115 Y.-J. Yuan, Z.-K. Shen, P. Wang, Z. Li, L. Pei, J. Zhong, Z. Ji, Z.-T. Yu and Z. Zou, *Appl. Catal., B*, 2020, **260**, 118179.
- 116 Y. F. Liu, M. F. He, R. Guo, Z. R. Fang, S. F. Kang, Z. Ma, M. D. Dong, W. L. Wang and L. F. Cui, *Appl. Catal., B*, 2020, **260**, 118137.
- 117 X.-B. Meng, J.-L. Sheng, H.-L. Tang, X.-J. Sun, H. Dong and F.-M. Zhang, *Appl. Catal., B*, 2019, **244**, 340–346.
- 118 B. Q. Xia, J. R. Ran, S. M. Chen, L. Song, X. L. Zhang, L. Q. Jing and S. Z. Qiao, *Nanoscale*, 2019, **11**, 8304–8309.
- 119 W. Chen, B. Han, C. Tian, X. Liu, S. Liang, H. Deng and Z. Lin, *Appl. Catal., B*, 2019, **244**, 996–1003.
- 120 Y. A. Wang, W. L. Zhen, Y. Q. Zeng, S. P. Wan, H. W. Guo, S. L. Zhang and Q. Zhong, *J. Mater. Chem. A*, 2020, **8**, 6034–6040.
- 121 J. T. Ren, Y. L. Zheng, K. Yuan, L. Zhou, K. Wu and Y. W. Zhang, *Nanoscale*, 2020, **12**, 755–762.
- 122 Q. Wang, G. Wang, X. Liang, X. Dong and X. Zhang, *Appl. Surf. Sci.*, 2019, **467–468**, 320–327.
- 123 S. Feng, R. Wang, S. Feng, Z. Zhang and L. Mao, *Res. Chem. Intermed.*, 2019, **45**, 1263–1279.
- 124 P. Li, J. Li, X. Feng, J. Li, Y. Hao, J. Zhang, H. Wang, A. Yin, J. Zhou, X. Ma and B. Wang, *Nat. Commun.*, 2019, **10**, 2177.
- 125 H. Liu, C. Xu, D. Li and H.-L. Jiang, *Angew. Chem., Int. Ed.*, 2018, **57**, 5379–5383.
- 126 S. J. Liu, C. Zhang, Y. D. Sun, Q. Chen, L. F. He, K. Zhang, J. Zhang, B. Liu and L. F. Chen, *Coord. Chem. Rev.*, 2020, **413**, 17.
- 127 Y. S. Wei, M. Zhang, R. Q. Zou and Q. Xu, *Chem. Rev.*, 2020, **120**, 12089–12174.
- 128 M. M. Wang, Y. F. Tang and Y. D. Jin, *ACS Catal.*, 2019, **9**, 11502–11514.
- 129 C. Wang, X. Liu, N. Keser Demir, J. P. Chen and K. Li, *Chem. Soc. Rev.*, 2016, **45**, 5107–5134.
- 130 S. Vajda and M. G. White, *ACS Catal.*, 2015, **5**, 7152–7176.
- 131 J. He, Y. Zhang, J. He, X. Zeng, X. Hou and Z. Long, *Chem. Commun.*, 2018, **54**, 8610–8613.
- 132 M. A. Nasalevich, M. G. Goesten, T. J. Savenije, F. Kapteijn and J. Gascon, *Chem. Commun.*, 2013, **49**, 10575–10577.
- 133 A. Cadiou, N. Kolobov, S. Srinivasan, M. G. Goesten, H. Haspel, A. V. Bavykina, M. R. Tchalala, P. Maity, A. Goryachev, A. S. Poryvaev, M. Eddaoudi, M. V. Fedin, O. F. Mohammed and J. Gascon, *Angew. Chem., Int. Ed.*, 2020, **59**, 13468–13472.
- 134 Y. Isaka, Y. Kawase, Y. Kuwahara, K. Mori and H. Yamashita, *Angew. Chem., Int. Ed.*, 2019, **58**, 5402–5406.
- 135 X.-K. Wang, J. Liu, L. Zhang, L.-Z. Dong, S.-L. Li, Y.-H. Kan, D.-S. Li and Y.-Q. Lan, *ACS Catal.*, 2019, **9**, 1726–1732.
- 136 J. Xu, Y. Qi, C. Wang and L. Wang, *Appl. Catal., B*, 2019, **241**, 178–186.
- 137 Q. Li, Z. Fan, L. Zhang, Y. Li, C. Chen, R. Zhao and W. Zhu, *J. Solid State Chem.*, 2019, **269**, 465–475.
- 138 L. Zhang, X. Shi, Z. Zhang, R. P. Kuchel, R. Namivandi-Zangeneh, N. Corrigan, K. Jung, K. Liang and C. Boyer, *Angew. Chem., Int. Ed.*, 2021, **60**, 5489–5496.
- 139 K. Gottschling, G. Savasci, H. Vignolo-Gonzalez, S. Schmidt, P. Mauker, T. Banerjee, P. Rovo, C. Ochsenfeld and B. V. Lotsch, *J. Am. Chem. Soc.*, 2020, **142**, 12146–12156.

- 140 W. Huang, N. Huber, S. Jiang, K. Landfester and K. A. I. Zhang, *Angew. Chem., Int. Ed.*, 2020, **59**, 18368–18373.
- 141 R. Y. Liu, K. T. Tan, Y. F. Gong, Y. Z. Chen, Z. E. Li, S. L. Xie, T. He, Z. Lu, H. Yang and D. L. Jiang, *Chem. Soc. Rev.*, 2021, **50**, 120–242.
- 142 K. Y. Geng, T. He, R. Y. Liu, S. Dalapati, K. T. Tan, Z. P. Li, S. S. Tao, Y. F. Gong, Q. H. Jiang and D. L. Jiang, *Chem. Rev.*, 2020, **120**, 8814–8933.
- 143 C. Krishnaraj, H. S. Jena, L. Bourda, A. Laemont, P. Pachfule, J. Roeser, C. V. Chandran, S. Borgmans, S. M. J. Rogge, K. Leus, C. V. Stevens, J. A. Martens, V. Van Speybroeck, E. Breynaert, A. Thomas and P. Van der Voort, *J. Am. Chem. Soc.*, 2020, **142**, 20107–20116.
- 144 N. Keller and T. Bein, *Chem. Soc. Rev.*, 2021, **50**, 1813–1845.
- 145 W. Q. Li, X. F. Huang, T. W. Zeng, Y. H. A. Liu, W. B. Hu, H. Yang, Y. B. Zhang and K. Wen, *Angew. Chem., Int. Ed.*, 2021, **60**, 1869–1874.
- 146 Z.-Z. Gao, Z.-K. Wang, L. Wei, G. Yin, J. Tian, C.-Z. Liu, H. Wang, D.-W. Zhang, Y.-B. Zhang, X. Li, Y. Liu and Z.-T. Li, *ACS Appl. Mater. Interfaces*, 2020, **12**, 1404–1411.
- 147 Z. Fu, X. Wang, A. M. Gardner, X. Wang, S. Y. Chong, G. Neri, A. J. Cowan, L. Liu, X. Li, A. Vogel, R. Clowes, M. Bilton, L. Chen, R. S. Sprick and A. I. Cooper, *Chem. Sci.*, 2020, **11**, 543–550.
- 148 Z. Y. Dong, L. Zhang, J. Gong and Q. Zhao, *Chem. Eng. J.*, 2021, **403**, 10.
- 149 X. X. Yu, Z. Z. Yang, B. Qiu, S. E. Guo, P. Yang, B. Yu, H. Y. Zhang, Y. F. Zhao, X. Z. Yang, B. X. Han and Z. M. Liu, *Angew. Chem., Int. Ed.*, 2019, **58**, 632–636.
- 150 X. Kang, X. W. Wu, X. Han, C. Yuan, Y. Liu and Y. Cui, *Chem. Sci.*, 2020, **11**, 1494–1502.
- 151 F. Strieth-Kalthoff and F. Glorius, *Chem*, 2020, **6**, 1888–1903.
- 152 A. Bhattacharjee, M. Sneha, L. Lewis-Borrell, G. Amoruso, T. A. A. Oliver, J. Tyler, I. P. Clark and A. J. Orr-Ewing, *J. Am. Chem. Soc.*, 2021, **143**, 3613–3627.
- 153 M. Yang, J. E. Yarnell, K. El Roz and F. N. Castellano, *ACS Appl. Energy Mater.*, 2020, **3**, 1842–1853.
- 154 D. Kong, M. Munch, Q. Qiqige, C. J. C. Cooze, B. H. Rotstein and R. J. Lundgren, *J. Am. Chem. Soc.*, 2021, **143**, 2200–2206.
- 155 J.-H. Shon, D. Kim, M. D. Rathnayake, S. Sittel, J. Weaver and T. S. Teets, *Chem. Sci.*, 2021, **12**, 4069–4078.
- 156 A. Shatskiy, A. Axelsson, E. V. Stepanova, J.-Q. Liu, A. Z. Temerdashev, B. P. Kore, B. Blomkvist, J. M. Gardner, P. Dinér and M. D. Kärkäs, *Chem. Sci.*, 2021, **12**, 5430–5437.
- 157 L.-L. Liao, G.-M. Cao, Y.-X. Jiang, X.-H. Jin, X.-L. Hu, J. J. Chruma, G.-Q. Sun, Y.-Y. Gui and D.-G. Yu, *J. Am. Chem. Soc.*, 2021, **143**, 2812–2821.
- 158 K.-K. Chen, S. Guo, H. Liu, X. Li, Z.-M. Zhang and T.-B. Lu, *Angew. Chem., Int. Ed.*, 2020, **59**, 12951–12957.
- 159 Y. Zhang, T. S. Lee, J. M. Favale, D. C. Leary, J. L. Petersen, G. D. Scholes, F. N. Castellano and C. Milsmann, *Nat. Chem.*, 2020, **12**, 345–352.
- 160 B. D. Ravetz, A. B. Pun, E. M. Churchill, D. N. Congreve, T. Rovis and L. M. Campos, *Nature*, 2019, **565**, 343–346.
- 161 A. Mahammed, K. P. Chen, J. Vestfrid, J. Z. Zhao and Z. Gross, *Chem. Sci.*, 2019, **10**, 7091–7103.
- 162 I. A. MacKenzie, L. Wang, N. P. R. Onuska, O. F. Williams, K. Begam, A. M. Moran, B. D. Dunietz and D. A. Nicewicz, *Nature*, 2020, **580**, 76–80.